

# INTERNATIONAL SOCIETY FOR SOIL MECHANICS AND GEOTECHNICAL ENGINEERING



*This paper was downloaded from the Online Library of the International Society for Soil Mechanics and Geotechnical Engineering (ISSMGE). The library is available here:*

<https://www.issmge.org/publications/online-library>

*This is an open-access database that archives thousands of papers published under the Auspices of the ISSMGE and maintained by the Innovation and Development Committee of ISSMGE.*

# The development of shaft friction for piles in sand overlying clay

## Le développement du frottement le long du fût des pieux dans un sable déposé sur une argile

G.O.ROWLANDS, Reader, Polytechnic of Wales, UK

R.DELPAK, Principal Lecturer, Polytechnic of Wales, UK

R.B.ROBINSON, Formerly Research Assistant, Polytechnic of Wales, UK

**SYNOPSIS:** The results of driving model piles 60 mm and 114 mm diameter through sand into clay are described. Data is provided on the interaction of the sand and the clay as the piles are driven, the generation of the pore pressure in the clay, the stresses at the interface and the soil displacement. The results show that except in the case of very short piles the contribution of shaft friction and adhesion is similar to that in single layers but the mechanism of load transfer is more complex.

### INTRODUCTION

This paper briefly describes some points observed when model segmental steel piles of different dimensions were installed in a clay underlying sand. The soil properties were:

A remoulded silty clay (Mercia Mudstone)

$W_l = 39\%$ ,  $I_p = 20\%$ ,

Placement water Content = 18%

Uniform Leighton Buzzard sand

$C_u = 1.79$   $C_c = 1.38$  Placed dry

The clay was placed at its optimum moisture content in a secondary tank 1.1 m diameter and 1.2 m high located in the base of a concrete tank 3 m diameter and 3 m deep. The larger tank was then filled with dry sand compacted under controlled conditions to a bulk density of  $1500 \text{ kg/m}^3$ . To minimise moisture migration from the clay a thin layer of sand was placed on the surface of the clay and then sprayed with a waterproof vinyl membrane. This procedure was discontinued in later tests as moisture migration proved to be negligible.

60 mm and 114 mm diameter steel piles were used. The 60 mm diameter pile was instrumented with piezoelectric washers, accelerometers and static axial load cells. It was driven dynamically using a pneumatically controlled hammer system. The 114 mm diameter pile was instrumented with a number of axial core load cells and sensitive boundary orthogonal stress transducers installed in the pile wall to monitor the development of normal (radial) and shear stresses. The pile was driven from the surface at a constant rate of penetration of 10.0 mm per minute. Details of the two systems are respectively given by Lake (1986) and Wersching (1987).

The results of two tests are considered in this paper: Test No 2 where a 60 mm pile was dynamically driven through the sand into the clay and Test No 5 where a 114 mm pile was driven at a constant rate of penetration in increments of approximately 100 mm. Each pile was then subjected to standard constant rate of penetration (CPR) and maintained load (ML) tests. The in-situ density of the sand was

monitored during placement and at selected points close to the pile towards the end of the testing programme using the plaster technique developed by Wersching (1983). The movement of the sand around the pile was continuously monitored using an arrangement of electrolytic levels and a system of small plates placed horizontally and vertically and linked to displacement transducers outside the tank.

### STRUCTURAL CHANGES IN THE CLAY

The structural changes observed in the clay due to pile installation are illustrated in Figure 1. The clay heaved slightly at the sand/clay interface. This was slightly more pronounced in the case of the dynamically driven pile. Heave extended for a distance of 2.75 B from the pile axis on each case. Surface heave in the sand, on the other hand, extended radially 4.0 B from the pile axis. The sand dragdown zones around the piles extended to depths of 2.5 B and 3.0 B respectively for the 60 mm and the 114 mm diameter piles. The displaced volume of clay was small in both cases due to the relatively short penetration into the clay. It is possible that heave was restricted by the sand overburden as the ratio of the heave to the displaced volume of clay was considerably lower than the values quoted for single layer conditions. The amount of sand dragdown would also tend to reduce this. There was clear evidence of a heavily distorted clay zone approximately 15 - 20 mm wide around both piles. The clay particles were clearly reorientated and all evidence of layering destroyed. It was also found to extend up through the dragdown sand zone and below the sand plug at the base of the pile. There was no evidence of sand in it and the impression is given that the sand plug at the pile tip is an isolated pocket. The sand plugs developed with each pile are illustrated in Figure 1. They appear as hemispherical cones slightly smaller in diameter than the pile shaft and extending 0.6 B below the pile tip. Both plugs were found to be completely saturated with water at the end of the test. This confirms their function as drainage outlets for the dissipation of pore pressure due to pile

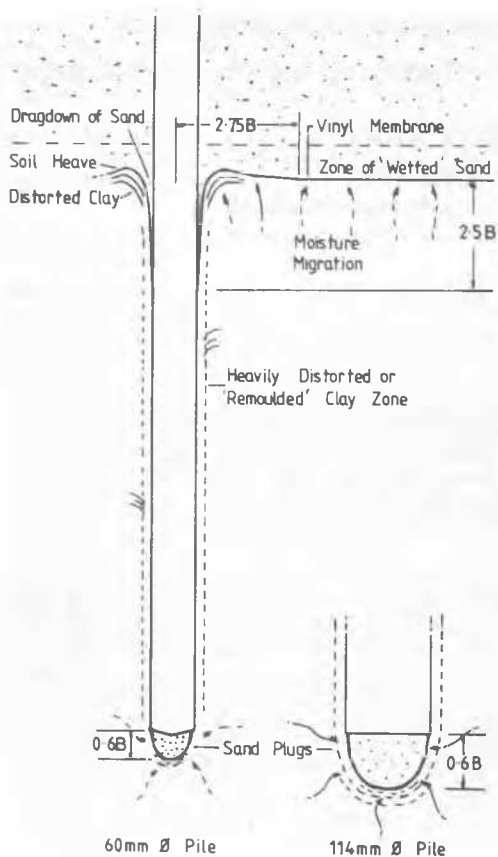


Figure 1 Structural Changes in the Clay due to Pile

driving and loading. This was also confirmed by a reduction in moisture in the clay around the plug observed at the end of the test. All these phenomena are unlikely to have a significant effect upon the shaft load carrying capacity except possibly in the case of very short piles. The end bearing resistance of the 114 mm pile in the sand did not appear to be influenced by the presence of the underlying clay until the pile tip was within 250 mm (2.2 B) above it. A significant decrease in the rate of increase in the value of the bearing capacity factor  $N$  below this depth was then observed although the maximum value occurred at 170 mm (1.5 B) above the clay. The shaft adhesion in the clay was mobilised as the pile penetrated beyond the dragdown zone and the value of  $N_c$  tended to 9.

#### DEVELOPMENT OF PORE PRESSURE

A continuous record of the pore pressure in the clay was provided by a series of piezometers installed at three different levels, with the lower level at the level of pile tips. The pattern was essentially similar in the two tests apart from the more rapid pore pressure build up during pile installation in the case of the 60 mm pile. This pile was fully driven in 4.5 hours whilst it took 8.5 hours to drive the 114 mm diameter pile. In Test 5 an increase in pore pressure

due to pile penetration of 200 mm (2 B approximately) into the sand whilst in Test 2 it occurred at a pile penetration of 240 mm (4 B approximately) into the sand. These observations are consistent with increases in the vertical pressure observed in pressure transducers located close to the pile at the sand/clay interface. Although the pore pressure build up occurred during most of the driving operation through the sand and the clay it appeared to be concentrated in a small area of the clay directly beneath the pile. This suggests that in a two layer system the interaction at the interface may restrict the transmission of stresses into the clay except in the region directly beneath the pile. The concentration of pore pressure close to the pile is also consistent with the concept that an expanding cavity develops only in the clay and the sand displaced by the pile is pushed out radially along the clay surface until either the pile or a sand plug ahead of it penetrates the clay.

However, a significant increase in pore water pressure was recorded by the piezometers as the piles penetrated the clay and passed the level of the piezometers. This suggests a high radial pressure gradient from the pile. The pore pressures recorded close to the level of the pile tip were consistently higher than those along the shaft. In the case of the 60 mm pile the maximum pore pressures at a radial distance of 1.5 B were equivalent to  $0.36 C_u$  and  $0.27 C_u$  opposite the base and shaft respectively. The corresponding values were  $0.56 C_u$  and  $0.34 C_u$  respectively for the 114 mm pile.

The maximum piezometer readings recorded during pile installation and subsequent (CRP) and (ML) tests were plotted against the logarithm of the radial distance from the pile axis in Figure 2. This relationship was found to be consistently linear for the whole embedded length of the piles and is of the form:

$$\Delta u = P C_u - R C_u \times \ln[2 r/B]$$

Where P and R define the magnitude of the pore pressure generated.

This relation is similar to the expression prescribed by Steenfelt et al (1979) of the form:

$$\Delta u = 4 C_u - 2 C_u \times \ln[2 r/B]$$

This expression was obtained from a series of tests when a 19 mm diameter pile was jacked into a reconstituted clay.

Figure 2 illustrates that the values of the P and R parameters were of the same order in the driving tests with a higher pore pressure being generated by the 114 mm pile. A similar linear relationship was obtained with the pile loading tests although the values of the parameters P and R and the pore pressures were considerably lower. The values of P and R were also substantially lower than the values given by Steenfelt et al. This is to be expected due to the low penetration, hence the low L/B ratio, into the clay as well as the additional drainage provided by the sand. In fact the pore expressed as a percentage of individual pile load increment.

An example of pore pressure dissipation rates after installation and loading tests is given in Figure 3. This data was obtained from a piezometer located at a radial distance of

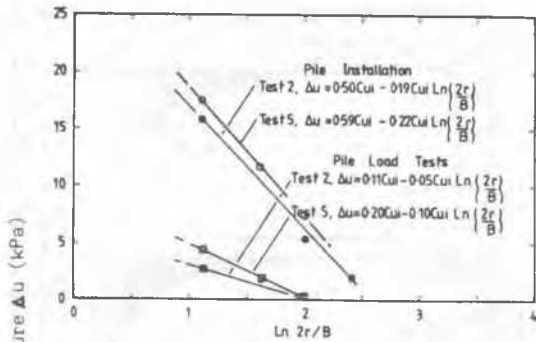


Figure 2. Logarithmic Radial Distribution of Excess Pore Water Pressure Generated within the Clay during Pile Installation and Load Tests

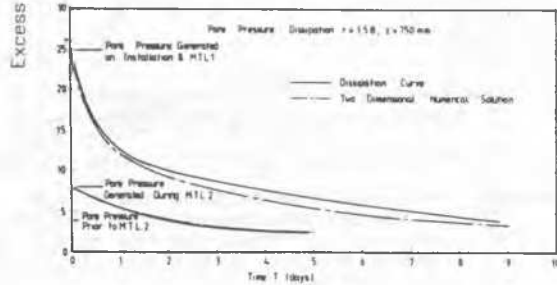


Figure 3 Dissipation of Excess Pore Water Pressure at a depth within the Clay equivalent to the Pile Base Level and at a radial distance  $r = 1.5 B$

1.5 B from the base of a 60 mm pile penetrating 750 mm into the clay 85 per cent pore pressure dissipation was achieved in 9 days after installation and an immediate (ML) test. A similar test for the 114 mm pile achieved the same degree of consolidation in 6.5 days. Possible explanation for the differences in dissipation rates are the different sizes of the sand plugs and the pile diameters.

A theoretical prediction of the pore pressure dissipation in the clay has been carried out using the explicit two dimensional finite difference method. The solution for a 60 mm pile assuming the sand/clay interface and the pile/clay surface to be free draining boundaries is also shown in Figure 3. This shows good agreement with the actual test data.

**STRESSES AT THE SAND/CLAY INTERFACE**

The normal and shear stress transducers located radially at selected points in the radial shear and the vertical effective stresses to be monitored as the piles were driven and subsequently test loaded. The full stress path could be evaluated in the case of Test 5 and is described in the following section. This was chosen in preference to Test 2 since only the residual stress path could be determined in the case of a dynamically driven pile. The development of

the effective vertical stress in the sand for a pile penetration of about 1000 mm (8.75 B) was consistent with the conventional Boussinesq bulb of pressure. This was approximately 250 mm above the sand/clay interface. But as the pile approached the clay interface and the sand cone penetrated the clay a significant increase in the vertical stress was observed consistent with the heave of the clay. This correlated with the vertical movement recorded in the region.

Similarly during the initial stages of pile penetration a build up of negative radial shear stress was recorded in the shear stress transducers. This is illustrated in Figure 4. This is consistent with the sand flowing radially outwards from the pile and confirmed by the movement of radial displacement plates located 125 mm above the sand/clay interface. As the pile and sand cone approached the clay and negative shear stress increased to a maximum or peak value and then reversed to a maximum positive shear and then decreased to a relatively constraint positive value as the pile penetrated further into the clay. This indicates a discontinuity in the lateral movement between the sand and clay (ie greater lateral movement occurring in the clay). A steady state of shear stress was reached with further pile penetration. Before the stress path was plotted it was assumed that the initial stresses at the interface level were

$\sigma_{ri} = K_o \sigma_{zi}$ , where  $\sigma_{zi}$  was the initial effective overburden stress. The resultant stress path plotted from the changes in these stresses formed failure envelopes with average angles of shearing resistance of 33 degrees. This is close to the measured  $\phi'$  for the sand and it confirms that shear failure was indeed occurring in the sand. Selected points on the stress path profile were plotted to enable the direction of the major principal stress  $\sigma_1$  in relation to pile embedment  $D_u$  to be determined. This is illustrated in Figure 5. The direction of this stress emanated from a point 0.6 B below the pile base ie close to the tip of the sand cone observed at the end of the test (Refer to Figure 1). It is possible that the sand plug would be more sharply pointed as shown in Figure 5 at this stage of the test.

As the radial shear failure was occurring in the reverse direction, when the pile and sand cone approached the clay layer, the major principal stress  $\sigma_1$  could be determined at this location. A reversal in the direction of  $\sigma_1$  occurred at this level and appeared to emanate from a point at 1.0 B below the pile base.

It appears from these results that shear failure occurred in the sand to a radial limit of 280 mm from the pile axis. At a radial distance of 480 mm no evidence of shear failure could be detected and the soil beyond this point probably tended towards the "at rest" condition with  $\sigma_{ri} = K_o \sigma_{zi}$ . Throughout the maintained load tests, the measured changes in effective vertical stress and radial shear stress were small but their values displayed trends consistent with the stress paths observed during pile driving.

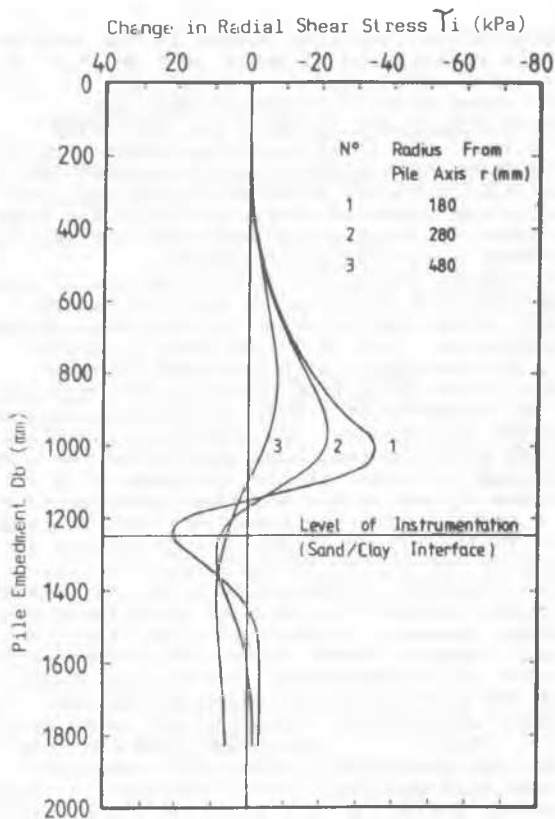


Figure 4 Radial Shear Stress History During Pile Installation.

VERTICAL AND RADIAL DISPLACEMENT OF THE SAND

The development of vertical and radial displacement of the sand around the pile and at the sand/clay interface was monitored by a system of electrolytic levels and metal plates linked to displacement transducers. A typical vertical displacement pattern during pile installation for the 114 mm pile is shown in Figure 6. This was fairly typical for both piles. In the initial stages of penetration, to a pile embedment depth of approximately 2.0 B, surface heave was evident to a radial distance of 310 mm (2.7 B) from the pile axis. The heave subsided with further penetration and a general downward vertical movement continued as the pile was driven. Within the body of the sand vertical movement increased progressively as the pile base approached the level of the instruments. This rate of movement decreased when the pile base was 2.0 B above the level of instrumentation and heave became apparent as the pile approached a level of 1.0 B. This may well be the onset of local rupture failure referred to by Robinsky and Morrison (1964). The heave extended a radial distance of approximately 4.0 B from the pile axis. It subsided when the pile base penetrated the clay but the sand continued to settle at a steady rate. The vertical movement at the sand/clay interface was generally similar to that detected in the sand. However, as the pile approached and penetrated the interface, the boundary effect

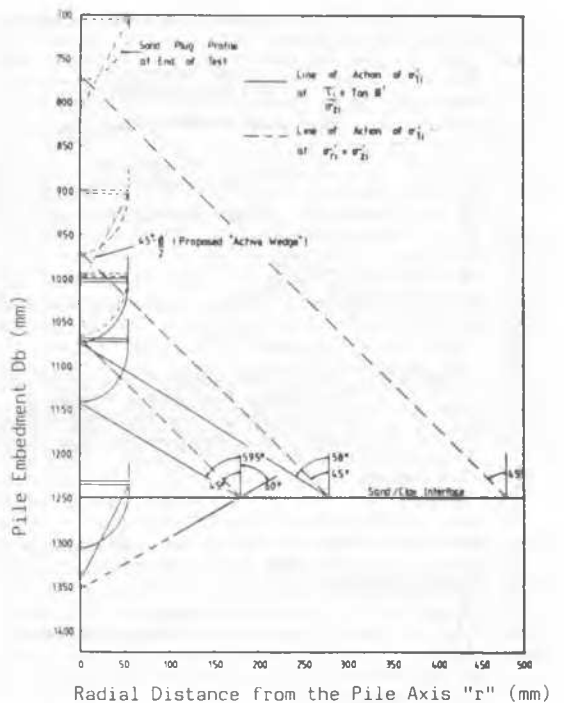


Figure 5 Soil/Pile Geometries associated with the maximum major effective principal stress and the onset of shear failure in a plane at a depth z = 1250 mm

and appreciable heave of the clay had a significant influence on the soil displacement. A resultant compressive strain within the sand was reflected by the development of an effective vertical stress at the interface. As heave subsided with further penetration vertical downward movement resumed as the pile penetrated into the clay.

The radial movement within the sand seemed to be independent of any heave in the clay but was dependant on the size of the pile. A significant feature here again, was that most of the radial movement occurred as the pile base approached the level of the instruments. It peaked when the pile was level with or just below the instruments and then reversed in direction towards the pile with further penetration. This relief in compressive strain was more pronounced in the case of the 60 mm diameter pile.

Figure 7 illustrates the peak radial displacement in the form 2R/B plotted against radial distance in the form 2r/B. The results were obtained from average peak values as the 60 mm and 114 mm diameter piles penetrated the sand. These values are compared with theoretical predictions of radial movements given by Wersching (1987) in the equation given below.

$$\frac{2R}{B} = C \times \frac{2r}{B} \dots \dots \dots (1)$$

where C = compaction factor

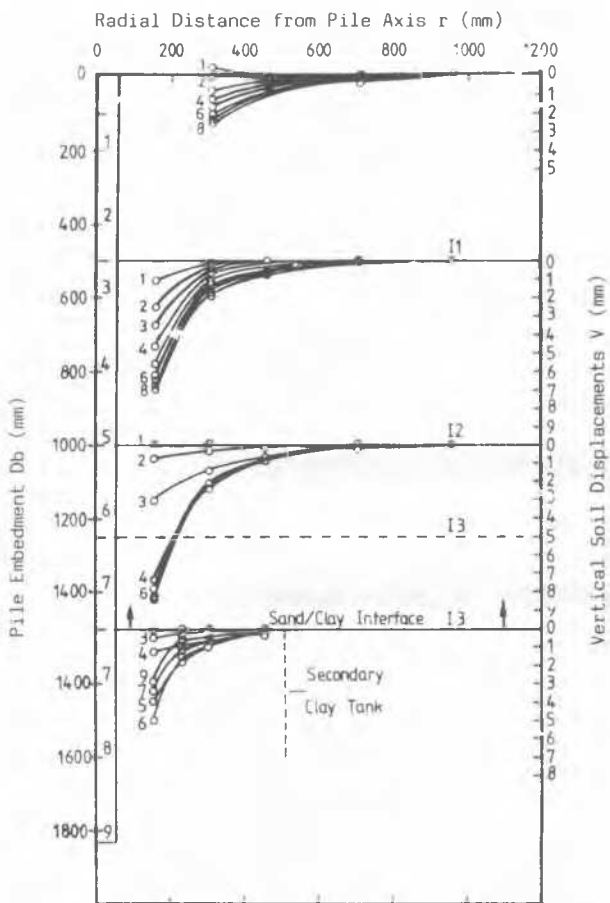


Figure 6 Development of Vertical Soil Displacements During Pile Installation

This is based upon equation (2) given by Randolph et al (1979) for  $\epsilon_z = \epsilon_v = 0$  and incorporating an empirical compaction factor (C).

$$\frac{2R}{B} = \left[ \left( \frac{2r}{B} \right)^2 + 1 \right]^{1/2} - \frac{2r}{B} \dots\dots(2)$$

Using the average values directly measured during the driving of the 60 mm and the 114 mm piles a compaction factor (C) of 0.85 gives a reasonable curve fit.

REFERENCES

Lake, G.C. (1986). The development of shaft friction and end bearing resistance for dynamically driven model piles, Ph.D.Thesis, C.N.A.A., The Polytechnic of Wales, United Kingdom.

Randolph, M.F., Steinfeld, J.S., and Wroth, C.P., (1979). The effect of pile type on design parameters for driven piles, Proc 7th European Conference, SMFE, 2, 107-114 Brighton.

Robinsky, E.I., and Morrison, C.F., (1964). Sand displacement and compaction around model friction piles, Canadian Geotechnical Journal, (1), 2, 81-93.

Steenfelt, J.S., Randolph, M.F., and Wroth, C.P., (1981). Instrumented model piles jacked into clay, Proc. 10th ICSMFE, 2, 857-864 Stockholm.

Wersching S.N., (1987). The development of shaft friction and end bearing for piles in homogeneous and layered soils, Ph.D. Thesis, C.N.A.A., The Polytechnic of Wales, United Kingdom.

Wersching, S.N., Delpak, R., and Rowlands, G.O. (1983). A method of estimating and in-situ density of dry uniformly graded sand under controlled conditions of placement, Geotechnical Testing Journal, ASTM, (6), 4, 196-200.

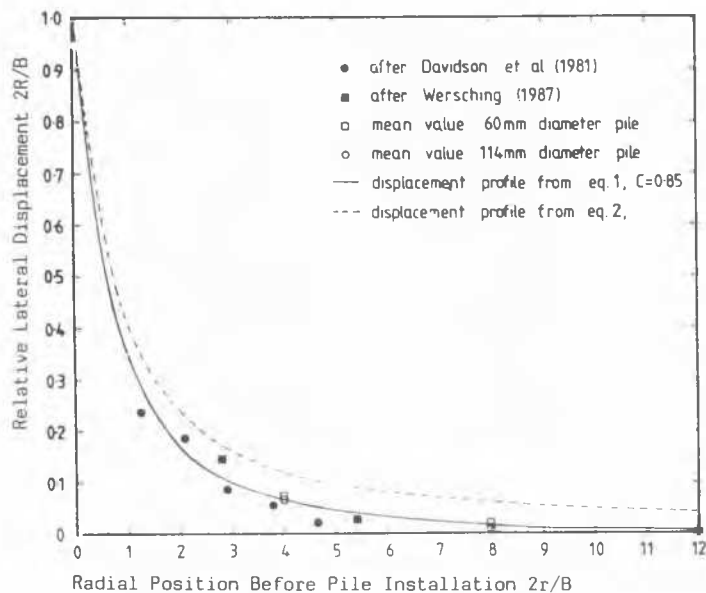


Figure 7 Normalised Radial Displacements In Loose Sand Due to Pile Installation